Rhenium tetrazolato complexes coordinated to thioalkyl-functionalised phenathroline ligands: synthesis, photophysical characterisation, and incubation in live HeLa cells

Melissa V. Werrett,[a] Phillip J. Wright,[a] Peter V. Simpson,[a] Paolo Raiteri,[a] Brian W. Skelton,[b] Stefano Stagni,[c] Alysia G. Buckley,[b] Paul J. Rigby,[b,*] Massimiliano Massi[a,*]

[a] *Department of Chemistry, Curtin University, Kent St., 6102 Bentley WA, Australia.*
[b] *Centre for Microscopy, Characterisation and Analysis, University of Western Australia, 6009 Crawley WA, Australia.*
[c] *Department of Industrial Chemistry "Toso Montanari", University of Bologna, viale del Risorgimento, Bologna 40126, Italy.*

Corresponding author email: paul.rigby@uwa.edu.au; m.massi@curtin.edu.au

Supplementary Information

^{1}H and ^{13}C NMR Spectra

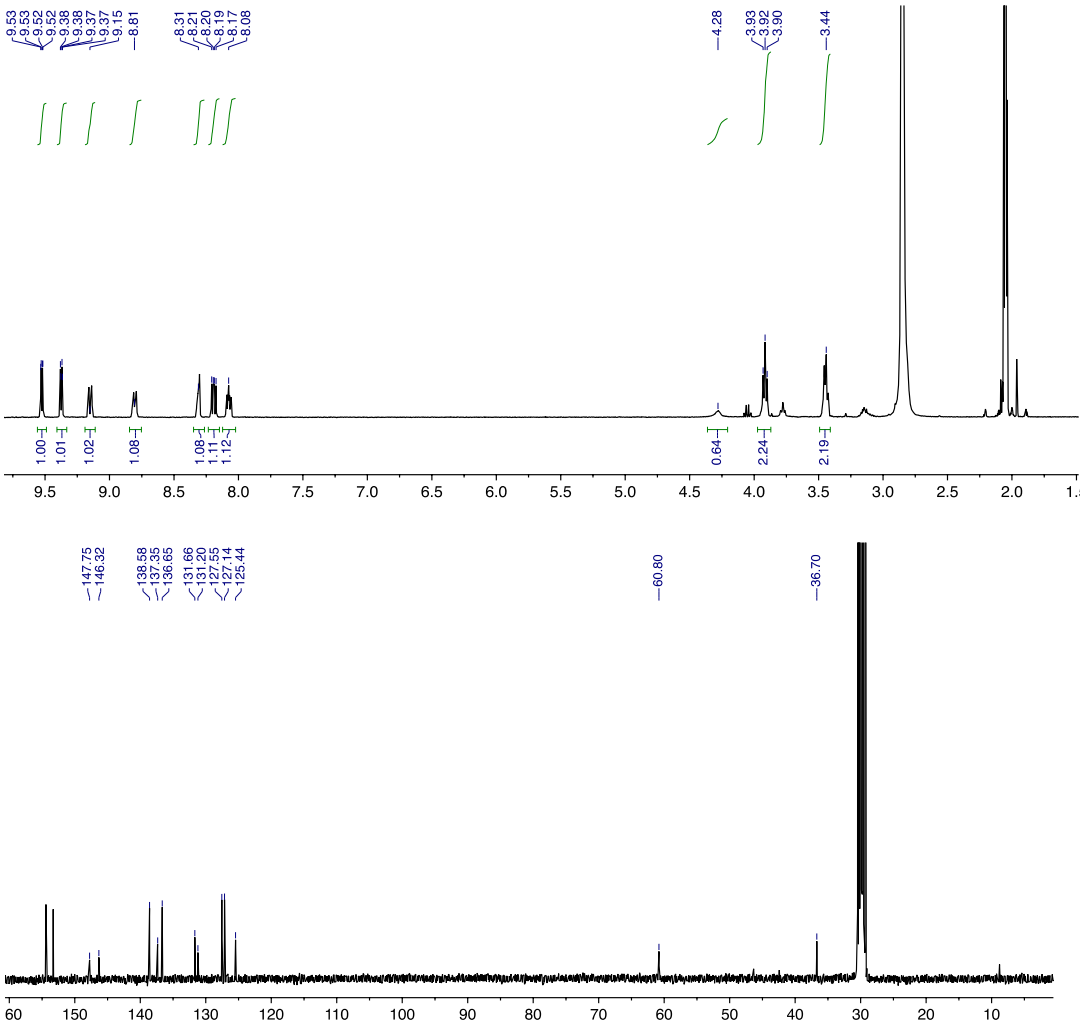

Figure S1. ^{1}H (top) and ^{13}C (bottom) NMR spectra of **S-ReCl.**

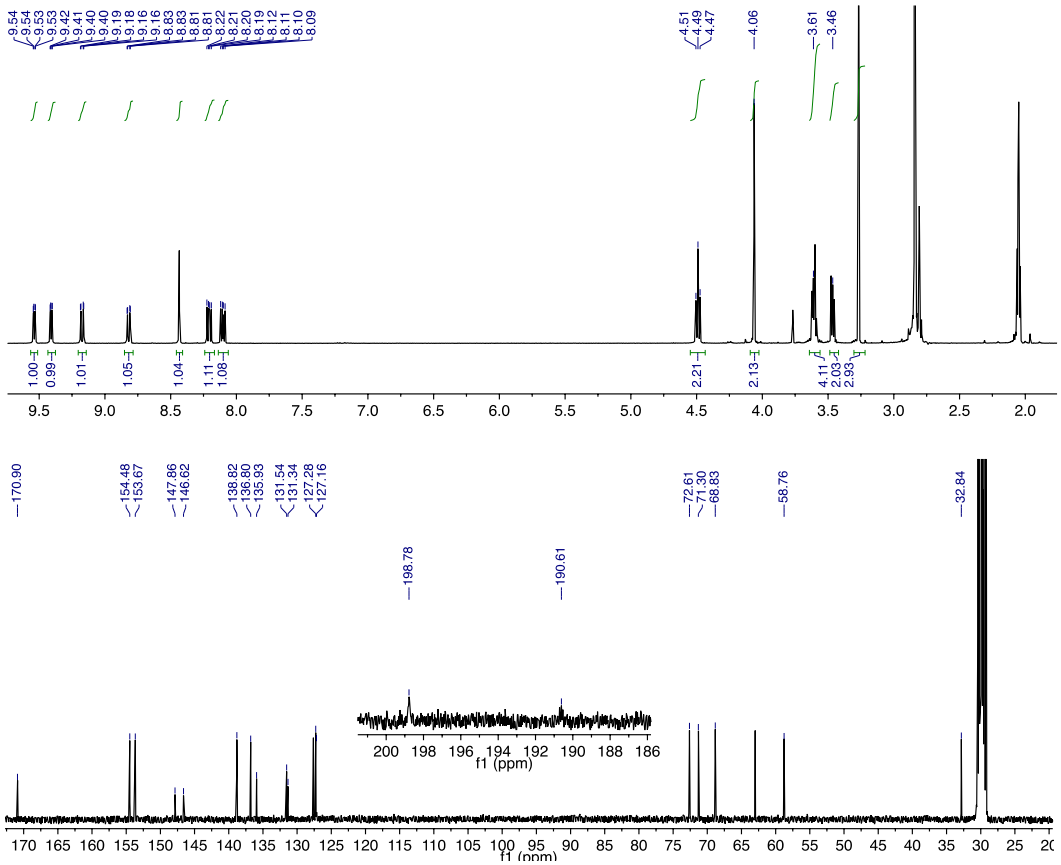

Figure S2. ^{1}H (top) and ^{13}C (bottom) NMR spectra of **EG-S-ReCl.**

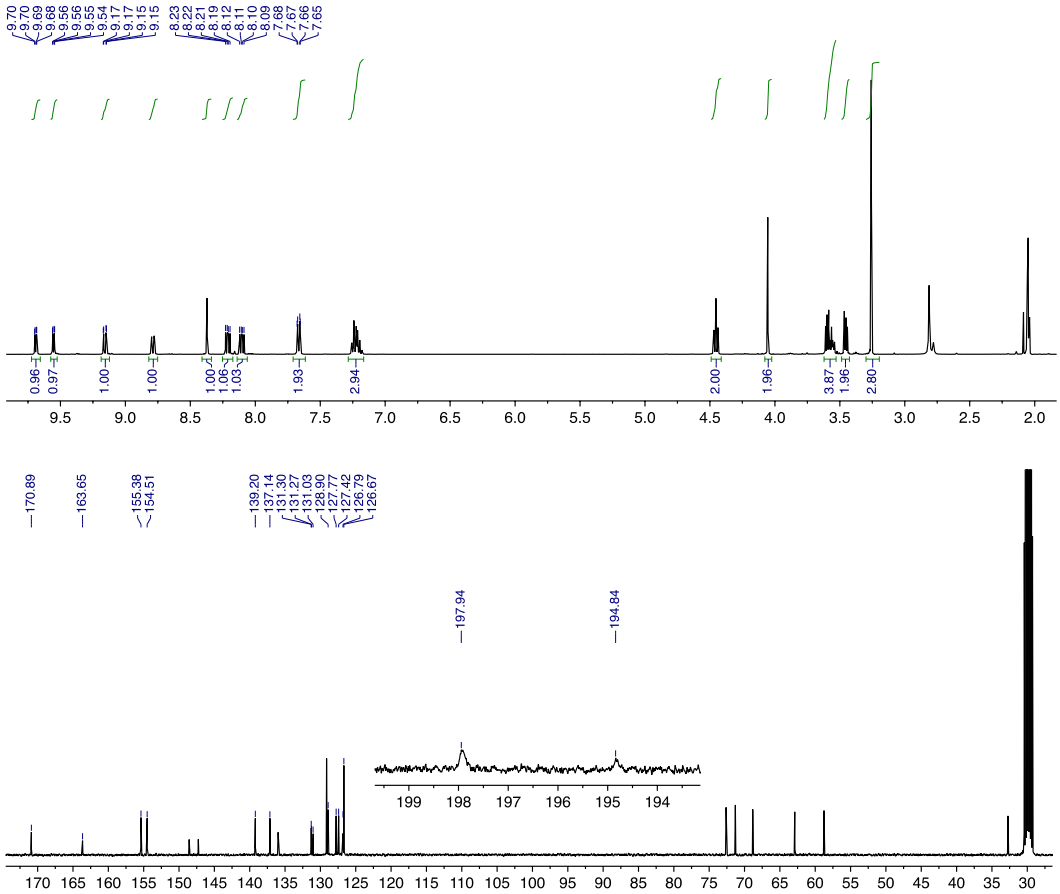

Figure S3. ^{1}H (top) and ^{13}C (bottom) NMR spectra of **EG-S-ReTPh.**

Table S1. Selected bond lengths [Å] and angles [°] for **S-ReCl**.

Re(1)-C(102)	1.899(4)
Re(1)-C(103)	1.921(4)
Re(1)-C(101)	1.926(4)
Re(1)-N(11)	2.176(3)
Re(1)-N(21)	2.183(3)
Re(1)-Cl(1)	2.4926(8)
N(11)-Re(1)-N(21)	75.49(10)
N(11)-Re(1)-Cl(1)	84.85(7)
N(21)-Re(1)-Cl(1)	82.38(7)

Table S2. Selected bond lengths [Å] and angles [°] for **EG-S-ReCl**.

Re(1)-C(103)	1.930(6)
Re(1)-C(101)	1.935(6)
Re(1)-C(102)	1.941(6)
Re(1)-N(121)	2.165(5)
Re(1)-N(111)	2.191(5)
Re(1)-Cl(1)	2.4866(15)
Re(2)-C(202)	1.927(6)
Re(2)-C(203)	1.936(7)
Re(2)-C(201)	1.938(7)
Re(2)-N(221)	2.164(5)
Re(2)-N(211)	2.176(5)
Re(2)-Cl(2)	2.4814(14)
C(103)-Re(1)-C(101)	87.3(3)
C(103)-Re(1)-C(102)	91.2(3)
C(101)-Re(1)-C(102)	87.8(3)
C(103)-Re(1)-N(121)	171.5(2)
C(101)-Re(1)-N(121)	97.9(2)
C(102)-Re(1)-N(121)	95.7(2)
C(103)-Re(1)-N(111)	99.6(2)
C(101)-Re(1)-N(111)	173.1(2)
C(102)-Re(1)-N(111)	92.8(2)
N(121)-Re(1)-N(111)	75.12(19)
C(103)-Re(1)-Cl(1)	90.40(19)
C(101)-Re(1)-Cl(1)	95.00(18)
C(102)-Re(1)-Cl(1)	176.86(18)
N(121)-Re(1)-Cl(1)	82.50(13)
N(111)-Re(1)-Cl(1)	84.27(13)
C(202)-Re(2)-C(203)	89.9(3)
C(202)-Re(2)-C(201)	87.6(3)
C(203)-Re(2)-C(201)	88.2(3)
C(202)-Re(2)-N(221)	94.6(2)
C(203)-Re(2)-N(221)	172.9(2)
C(201)-Re(2)-N(221)	97.5(2)
C(202)-Re(2)-N(211)	93.0(2)
C(203)-Re(2)-N(211)	98.9(2)

C(201)-Re(2)-N(211)	172.9(2)
N(221)-Re(2)-N(211)	75.38(19)
C(202)-Re(2)-Cl(2)	175.9(2)
C(203)-Re(2)-Cl(2)	92.7(2)
C(201)-Re(2)-Cl(2)	95.69(18)
N(221)-Re(2)-Cl(2)	82.60(13)
N(211)-Re(2)-Cl(2)	83.46(13)

TDDFT

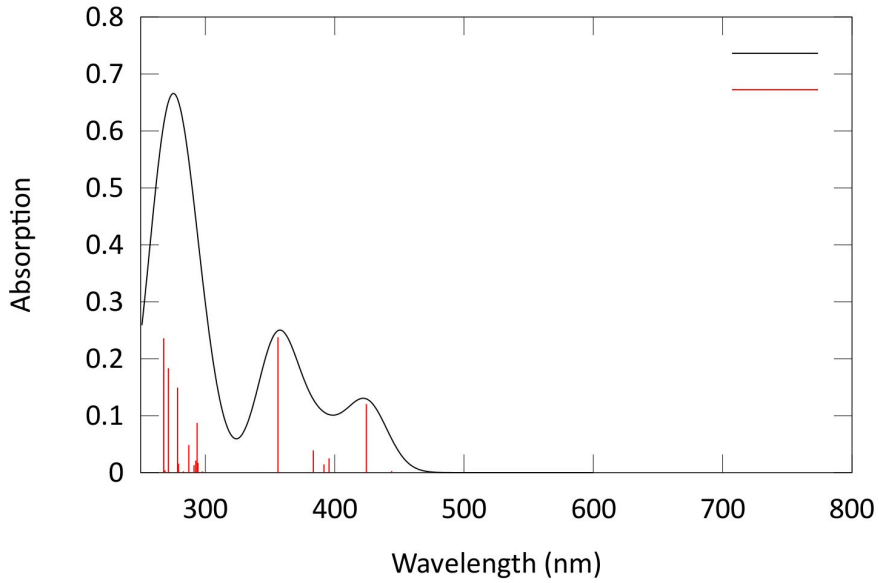

Figure S4. Simulated absorption spectrum of **S-ReCl**.

Table S3. Calculated electronic transitions for **S-ReCl**.

Wavelength	Intensity	Levels	Character
424.53 nm	**0.1204**	**HOMO-1 -> LUMO**	**96.7 %**
356.16 nm	**0.2376**	**HOMO-2 -> LUMO+1**	**89.3 %**
293.66 nm	0.0874	HOMO-6 -> LUMO	4.3 %
		HOMO-4 -> LUMO	63.0 %
292.61 nm	0.0211	HOMO-6 -> LUMO	2.1 %
		HOMO-4 -> LUMO	10.1 %
		HOMO-2 -> LUMO+3	4.9 %
		HOMO-1 -> LUMO+3	59.8 %
		HOMO -> LUMO+2	15.1 %
		HOMO -> LUMO+3	3.4 %
291.30 nm	0.0132	HOMO-5 -> LUMO	80.1 %
		HOMO-4 -> LUMO	2.6 %
		HOMO-4 -> LUMO+1	3.9 %
		HOMO-1 -> LUMO+2	7.2 %
278.55 nm	0.1494	HOMO-7 -> LUMO	2.1 %
		HOMO-6 -> LUMO	43.7 %
		HOMO-5 -> LUMO	2.3 %
		HOMO-5 -> LUMO+1	24.0 %
		HOMO-4 -> LUMO+1	4.9 %
		HOMO-2 -> LUMO+2	10.5 %
		HOMO -> LUMO+2	2.4 %
		HOMO -> LUMO+4	2.1 %

271.44 nm	0.1834	HOMO-7 -> LUMO	3.0 %
		HOMO-6 -> LUMO+1	17.9 %
		HOMO-5 -> LUMO+1	2.1 %
		HOMO-4 -> LUMO+1	29.0 %
		HOMO-2 -> LUMO+2	39.9 %
		HOMO-1 -> LUMO+2	2.0 %
		HOMO-1 -> LUMO+4	2.5 %
267.84 nm	0.2359	HOMO-7 -> LUMO+1	2.4 %
		HOMO-6 -> LUMO	16.5 %
		HOMO-5 -> LUMO+1	63.4 %
		HOMO-4 -> LUMO	4.8 %
		HOMO-4 -> LUMO+1	2.6 %
		HOMO-3 -> LUMO+2	2.0 %
		HOMO-3 -> LUMO+2	2.0 %

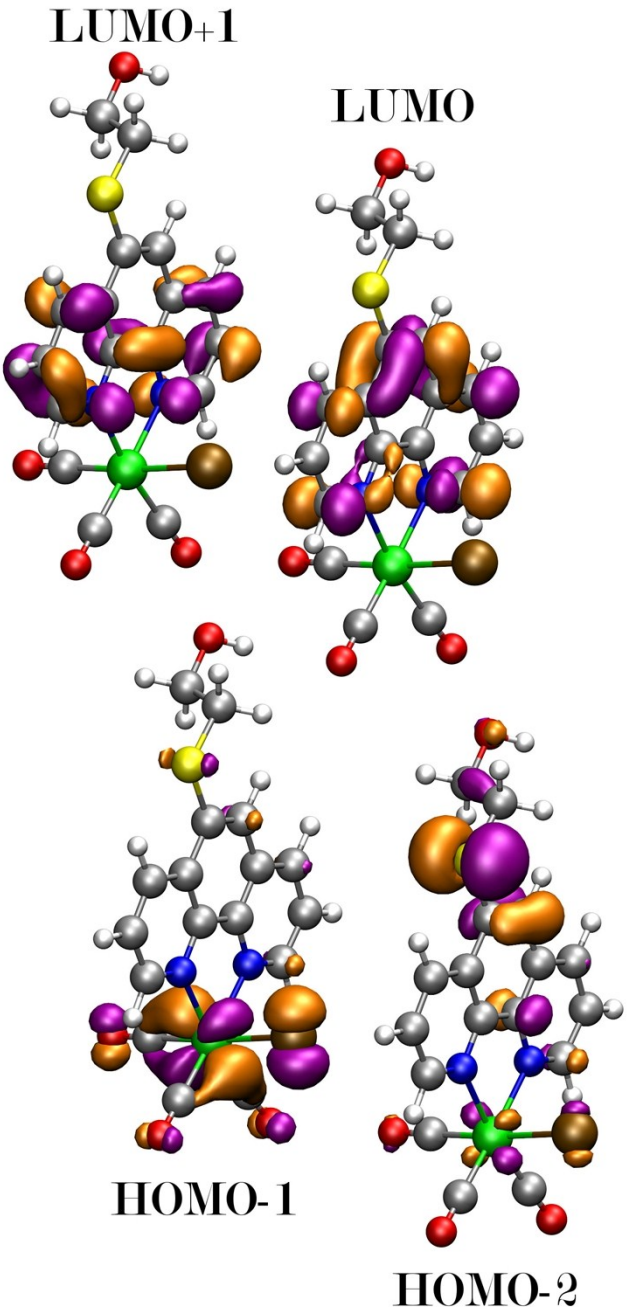

Figure S5. Selected orbital contours for **S-ReCl**.

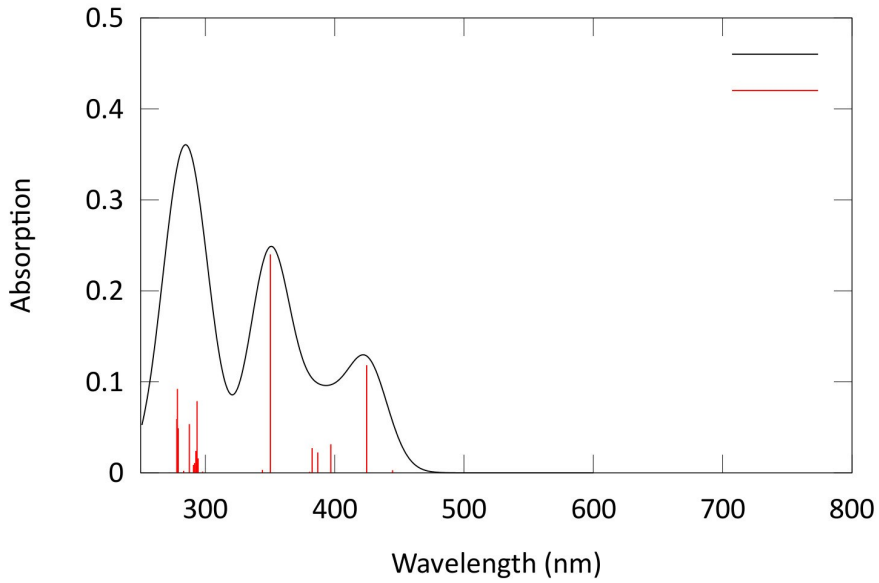

Figure S6. Simulated absorption spectrum of **EG-S-ReCl**.

Table S3. Calculated electronic transitions for **EG-S-ReCl**.

Wavelength	Intensity	Levels	Character
424.75 nm	**0.1183**	**HOMO-1 -> LUMO**	**96.6 %**
397.01 nm	0.0314	HOMO -> LUMO+1	94.8 %
350.29 nm	**0.2401**	**HOMO-2 -> LUMO+1**	**91.4 %**
293.61 nm	0.0788	HOMO-8 -> LUMO	4.6 %
		HOMO-6 -> LUMO	59.6 %
		HOMO-1 -> LUMO+3	22.1 %
292.69 nm	0.0241	HOMO-6 -> LUMO	13.2 %
		HOMO-1 -> LUMO+3	57.4 %
		HOMO -> LUMO+2	14.0 %
287.65 nm	0.0536	HOMO-7 -> LUMO	12.7 %
		HOMO-6 -> LUMO	2.4 %
		HOMO-1 -> LUMO+2	70.6 %
		HOMO -> LUMO+3	7.6 %
279.03 nm	0.0490	HOMO-8 -> LUMO	29.7 %
		HOMO-7 -> LUMO+1	8.9 %
		HOMO-6 -> LUMO+1	21.5 %
		HOMO-4 -> LUMO+1	28.3 %
		HOMO-2 -> LUMO+2	5.2 %
278.41 nm	0.0922	HOMO-10 -> LUMO	3.5 %
		HOMO-8 -> LUMO	10.9 %
		HOMO-7 -> LUMO	2.7 %
		HOMO-7 -> LUMO+1	10.8 %
		HOMO-6 -> LUMO+1	39.3 %
		HOMO-4 -> LUMO+1	5.3 %

		HOMO-2 -> LUMO+2	17.9 %
		HOMO-1 -> LUMO+2	2.7 %
277.95 nm	0.0592	HOMO-8 -> LUMO	19.9 %
		HOMO-7 -> LUMO+1	8.8 %
		HOMO-4 -> LUMO+1	65.9 %

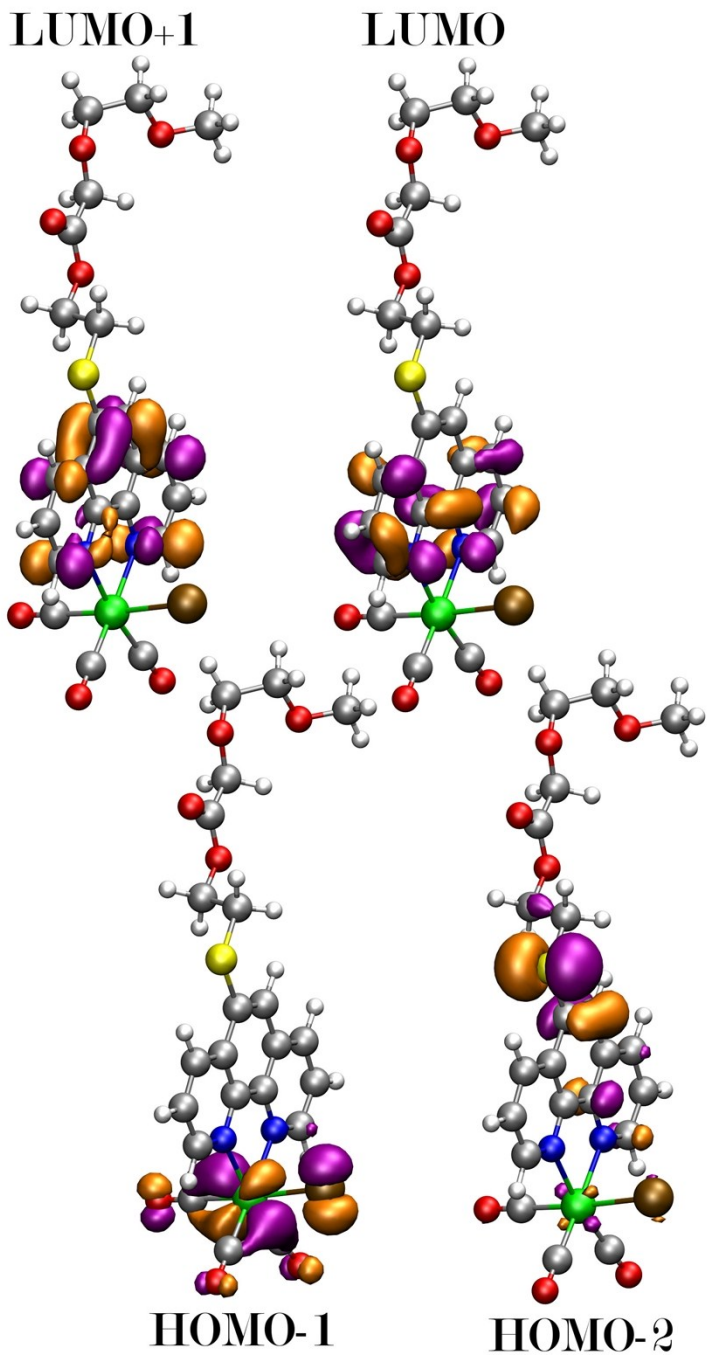

Figure S7. Selected orbital contours for **EG-S-ReCl**.

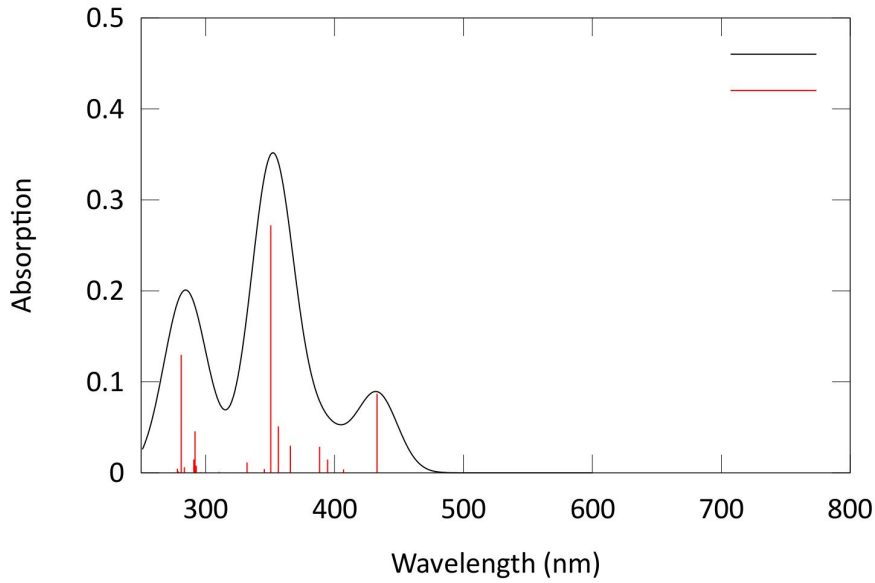

Figure S8. Simulated absorption spectrum of **EG-S-ReTPh**.

Table S4. Calculated electronic transitions for **EG-S-ReTPh**.

Wavelength	Intensity	Levels	Character
432.98 nm	**0.0870**	**HOMO -> LUMO**	**96.3 %**
388.38 nm	0.0286	HOMO-4 -> LUMO	2.4 %
		HOMO-2 -> LUMO	82.1 %
365.72 nm	0.0297	HOMO-4 -> LUMO	5.9 %
		HOMO-2 -> LUMO+1	7.0 %
		HOMO-1 -> LUMO+1	83.6 %
356.47 nm	0.0511	HOMO-4 -> LUMO	70.9 %
		HOMO-3 -> LUMO	11.2 %
350.55 nm	**0.2720**	**HOMO-2 -> LUMO+1**	**80.2 %**
		HOMO-4 -> LUMO	5.5 %
		HOMO-4 -> LUMO+1	4.6 %
		HOMO-9 -> LUMO	2.1 %
		HOMO-1 -> LUMO+1	3.8 %
332.13 nm	0.0114	HOMO-4 -> LUMO+1	84.2 %
		HOMO-3 -> LUMO+1	8.2 %
		HOMO-2 -> LUMO+1	4.4 %
291.78 nm	0.0456	HOMO-8 -> LUMO	72.8 %
		HOMO-6 -> LUMO	11.7 %
		HOMO -> LUMO+2	10.3 %
290.86 nm	0.0147	HOMO-8 -> LUMO	13.7 %
		HOMO -> LUMO+2	79.4 %
281.07 nm	0.1296	HOMO-9 -> LUMO	48.1 %
		HOMO-2 -> LUMO+2	3.1 %
		HOMO-1 -> LUMO+2	34.1 %
		HOMO-1 -> LUMO+5	2.2 %

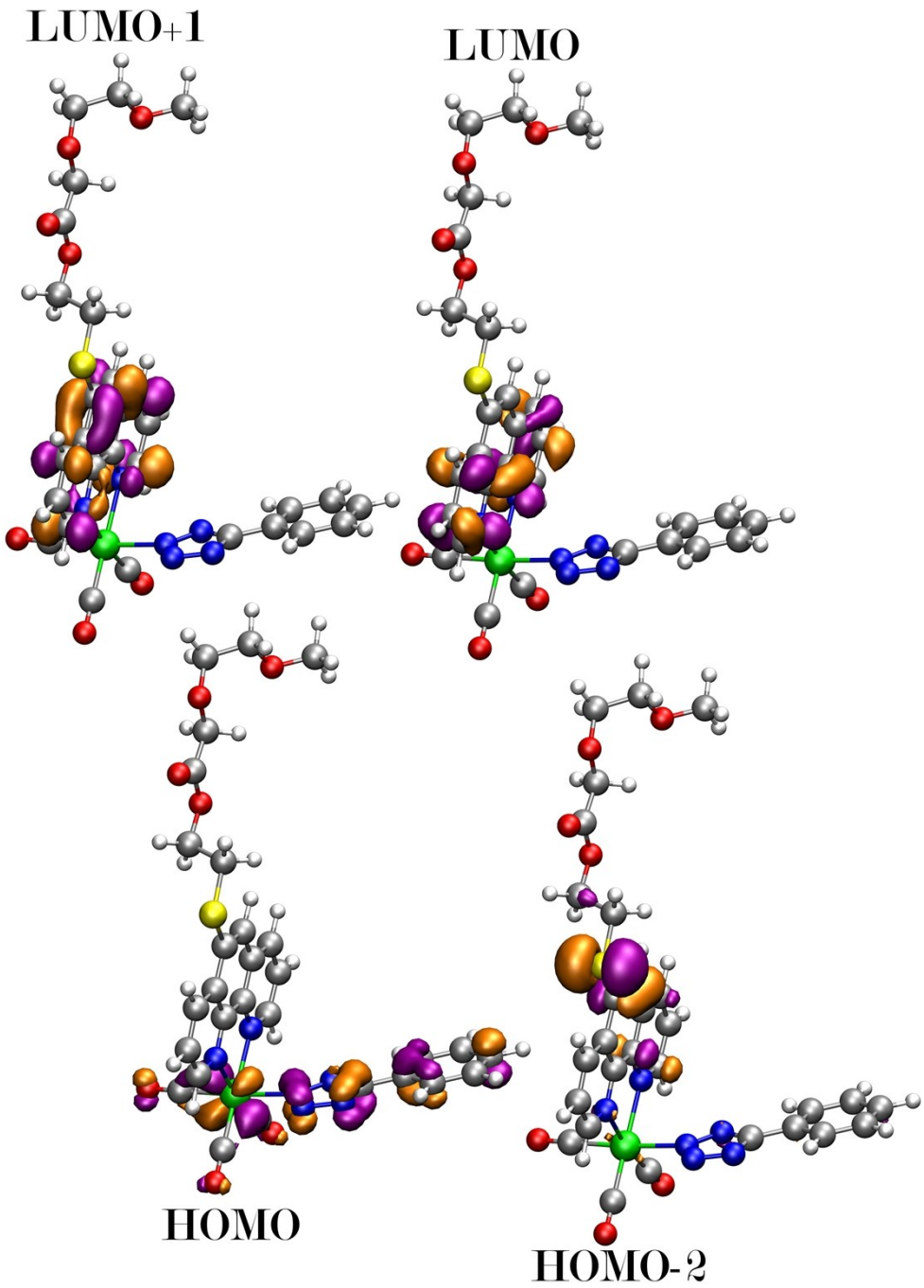

Figure S8. Selected orbital contours for **EG-S-ReTPh**.

Confocal Images of Live HeLa Cells

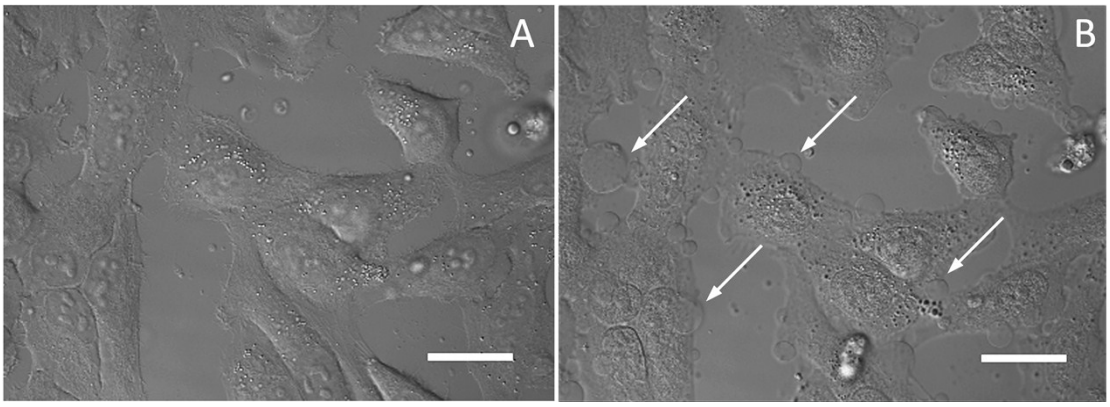

Figure S9. DIC images of HeLa Cells before (A) and after (B) the direct addition of DMSO to the culture. The arrows point to the presence of blebs in image B. Scale bar = 25 μm.

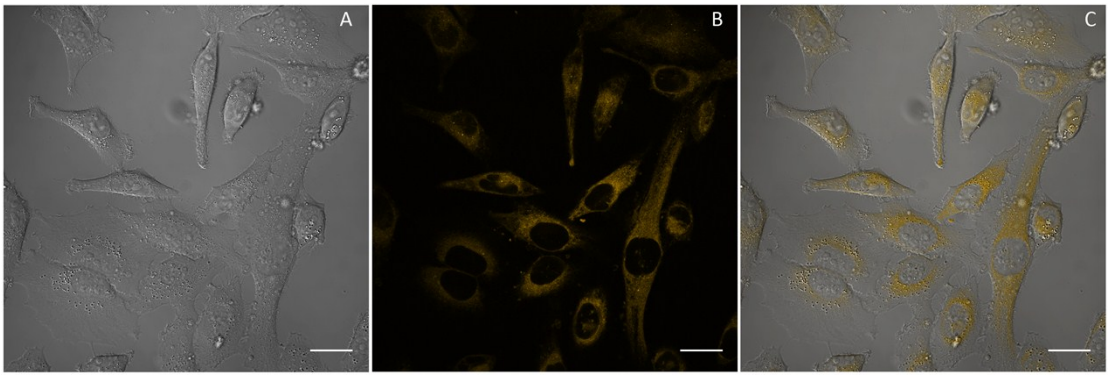

Figure S10. HeLa cells incubated with **ReTBz**. DIC image (A) shows the strucutral integrity of the cells, whereas the luminescence (B) and merged (C) images illustrate cellular uptake and perinuclear localisation. Scale bar = 25 μm

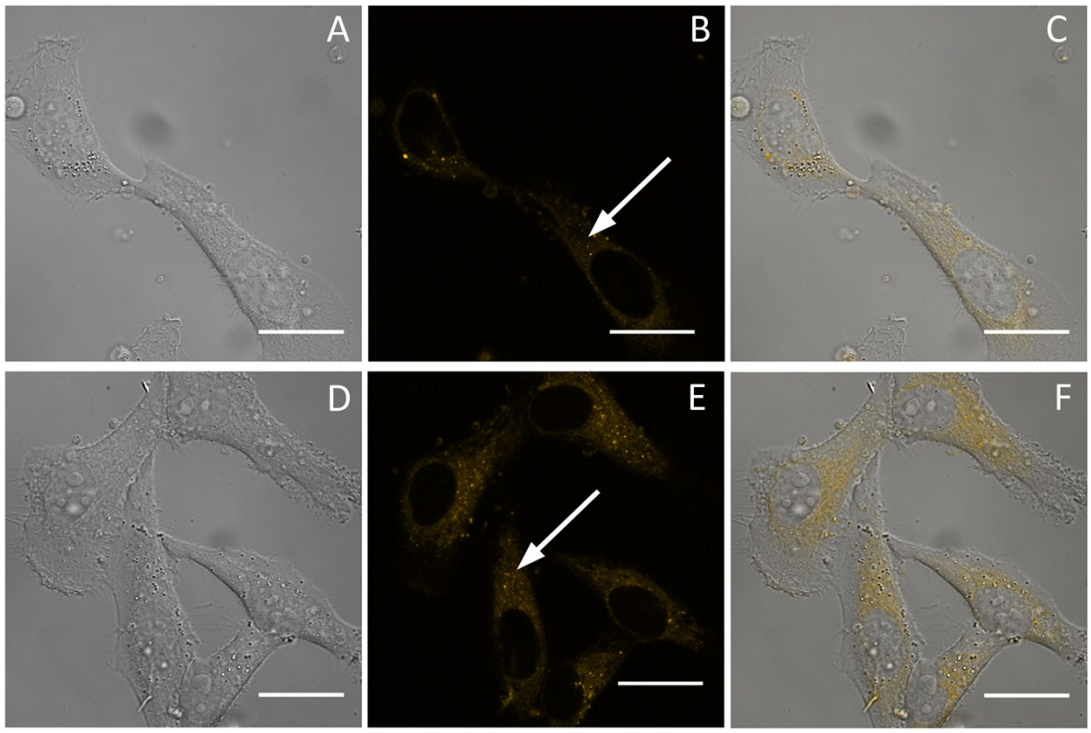

Figure S11. HeLa cells incubated with **S-ReCl** (A-C) and **EG-S-ReCl** (D-F). DIC images (A and D) show the structural integrity of cells, whereas luminescence (B and E) and merged images (C and F) illustrate the uptake and perinuclear localisation. Scale bar = 25 μm. The white arrows indicate the point chosen for the spectral detection.

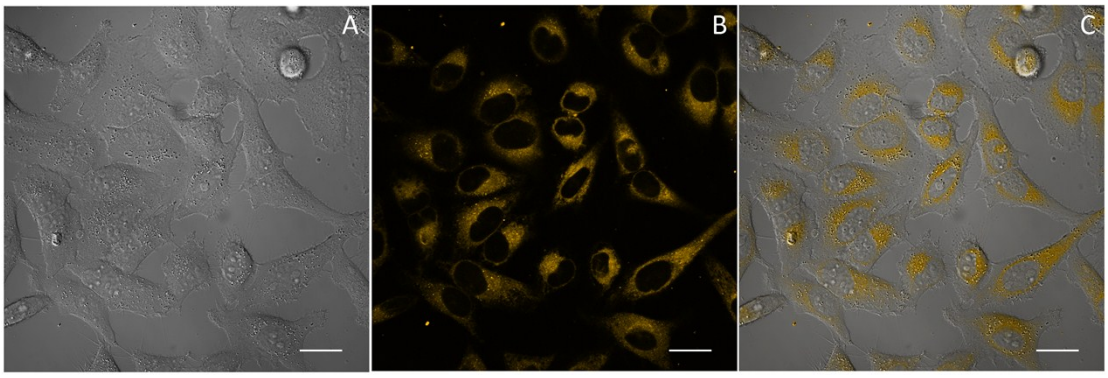

Figure S12. HeLa cells incubated with **EG-S-ReTPh**. DIC image (A) shows the structural integrity of HeLa cells, whereas the luminescence (B) and merged images (C) illustrate the uptake and perinuclear localisation. Scale bar = 25 μm.

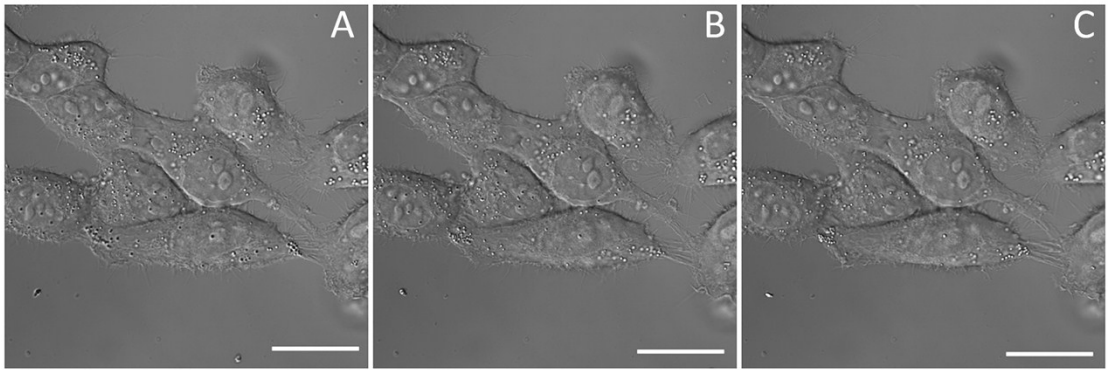

Figure S13. DIC images from a five minute time laspe of untreated HeLa cells. Cell medium contains 0.5% DMSO. DIC images show the structural integrity of HeLa cells where A: t=0 (A), t=2.5 min (B) and t=5 min (C). Scale bar = 25 μm.

Spectral Detection from HeLa cells

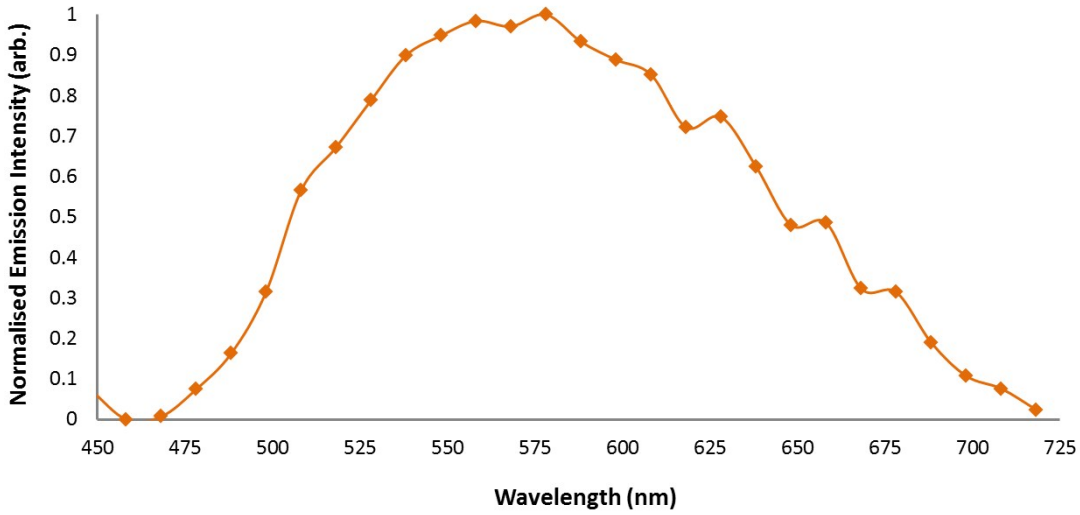

Figure S14. Spectral profile of **ReTBz** from the perinuclear region of live HeLa cells.

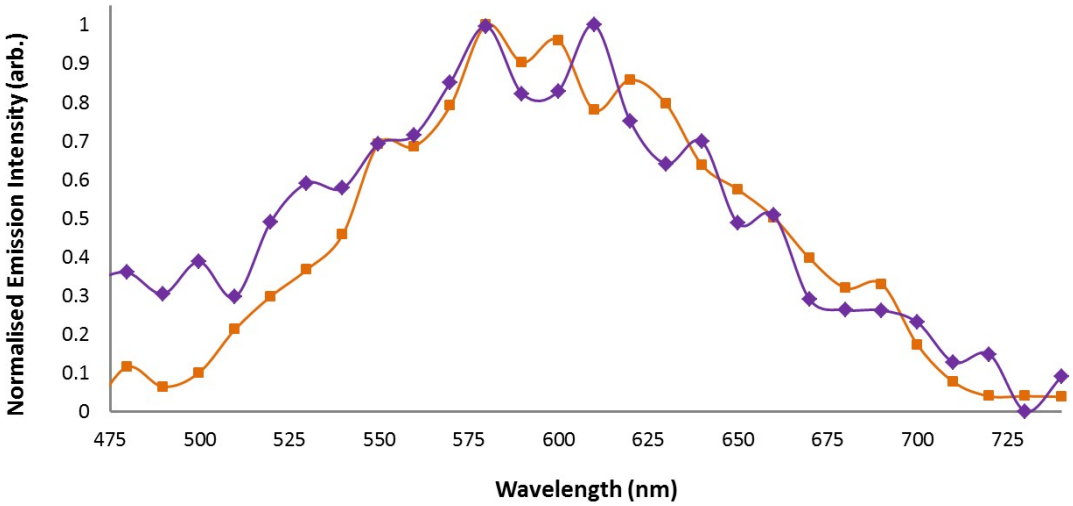

Figure S15. Spectral profiles of **S-ReCl** (orange) and **EG-S-ReCl** (blue) from the perinuclear region of live HeLa cells.

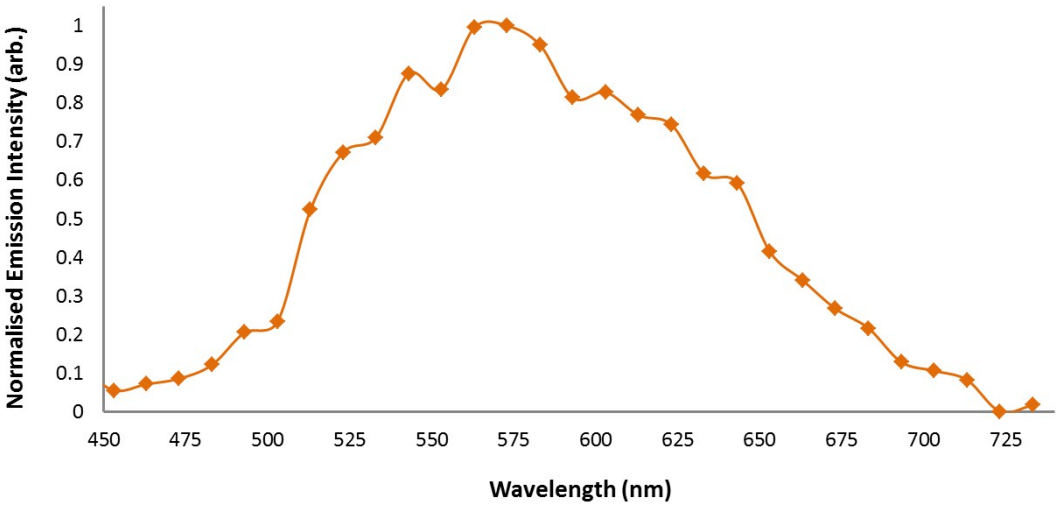

Figure S16. Spectral profile of **EG-S-ReTPh** from the perinuclear region of live HeLa cells.